Published in final edited form as:
Biomacromolecules. 2010 November 8; 11(11): 2976–2984. doi:10.1021/bm1007794.

Adhesive Performance of Biomimetic Adhesive-Coated Biologic Scaffolds

John L. Murphy, **Laura Vollenweider**, **Fangmin Xu**, and **Bruce P. Lee***
Nerites Corporation, Madison, WI

Abstract

Surgical repair of a discontinuity in traumatized or degenerated soft tissues is traditionally accomplished using sutures. A current trend is to reinforce this primary repair with surgical grafts, meshes, or patches secured with perforating mechanical devices (i.e., sutures, staples, or tacks). These fixation methods frequently lead to chronic pain and mesh detachment. We developed a series of biodegradable adhesive polymers that are synthetic mimics of mussel adhesive proteins (MAPs), composed of 3,4-dihydroxyphenylalanine (DOPA)-derivatives, polyethylene glycol (PEG), and polycaprolactone (PCL). These polymers can be cast into films, and their mechanical properties, extent of swelling, and degradation rate can be tailored through the composition of the polymers as well as blending with additives. When coated onto a biologic mesh used for hernia repair, these adhesive constructs demonstrated adhesive strengths significantly higher than fibrin glue. With further development, a pre-coated bioadhesive mesh may represent a new surgical option for soft tissue repair.

Keywords

biomimetic material; tissue adhesive; surgical mesh; multiblock copolymer; DOPA

1 Introduction

Surgical repair and reconstruction of traumatized or degenerated soft tissues occurs frequently in medicine. While the discontinuity in the soft tissue is traditionally closed with sutures, the use of surgical meshes or patches to reinforce suture closure is becoming popular in various surgical procedures such as hernia repair,[1–3] tendon repair,[4, 5] cardiovascular surgery,[6] and dural repair.[7] Fixation of these prosthetic materials is typically achieved through the use of sutures, staples, or tacks. While such perforating fixation devices have demonstrated success in immobilizing surgical meshes, they are also a source of complications. For example, in hernia repair, mechanical fixation methods may be the source of neural irritation and persistent pain.[8–11] In tendon reconstruction, on the other hand, surgical repairs often fail as sutures pull out through the tendinous tissue with loading.[12, 13]

In order to reduce these complications, several investigators have used fibrin sealant for mesh fixation.[14–17] While some level of success has been demonstrated, it has also been shown that the weak adhesive strength of fibrin sealants could not adequately prevent mesh migration and detachment in a number of applications.[14, 15] In addition, using a fibrin sealant requires mixing its constituents before application, which complicates intraoperative workflow and lengthens the time of surgery. While others have used stronger tissue

*Corresponding author: Nerites Corporation, 505 S Rosa Road, Suite 123, Madison, WI, 53719. TEL: (608) 335-5285 FAX: (608) 443-2440 b-lee@nerites.com.

adhesives such as cyanoacrylate[18] and gelatin-resorcinol-formaldehyde (GRF),[19] these adhesives have safety concerns[20–22] and can dramatically alter the biomechanical properties of the reinforced tissues.[18]

To improve the efficacy of mesh use for soft tissue reconstruction, we coated water-resistant, synthetic adhesives inspired by marine mussels onto biologic meshes to create a bioadhesive construct which can potentially eliminate complications associated with perforation-based fixation devices. The adhesive polymers described herein are synthetic mimics of mussel adhesive proteins (MAPs) that enable mussels to anchor to a variety of surfaces in wet, saline, turbulent environments.[23, 24] One unique structural feature of MAPs is the presence of 3,4-dihydroxyphenylalanine (DOPA),[23] a catecholic amino acid arising from post-translational modification of tyrosine in the presence of enzymes such as tyrosinase.[25] DOPA is believed to fulfill a dual role as a surface adhesion promoter and a crosslinking precursor.[26–28] When DOPA and its derivatives are chemically coupled to synthetic polymers, these synthetic mimics demonstrate strong moisture-resistant adhesive properties to various substrates, including titanium,[29, 30] mucin,[31, 32] soft tissue,[33, 34] and bone.[35]

In this paper, we describe the synthesis of a new series of adhesive polymers composed of DOPA derivatives chemically modified onto biodegradable and biocompatible multiblock copolymers consisting of poly(ethylene glycol) (PEG) and polycaprolactone (PCL). These polymers were cast into thin films and their tensile mechanical properties, equilibrium swelling properties, and *in vitro* degradation profiles were characterized. As a demonstration of forming adhesive-coated meshes, these adhesive polymer films were solvent casted onto bovine pericardium, as well as three representative commercially available biologic meshes (Permacol™, Covidien; CollaMend®, C.R. Bard; Surgisis®, Cook Biotech) used in hernia repair (Figure 1). Biologic mesh materials were chosen in this study because they can potentially provide a scaffold that promotes rapid tissue ingrowth, resulting in an organized collagenous tissue.[36–39] In addition, biologic meshes generate a reduced inflammatory response, fewer infections, and fewer post-surgical adhesions to surrounding tissues than do synthetic meshes. The adhesive properties of these adhesive-coated biologic meshes were determined using lap shear and burst tests.

2 Experimental

Here, we describe the procedures for the preparation of two adhesive polymers, **AP1** and **AP2** (Schemes 1 and 2, respectively), which were synthesized utilizing two linear bi-functional PCL precursors, **PCL1250-diSA** and **PCL2000-diGly**, respectively. These polymers were characterized using nuclear magnetic resonance (NMR), UV-vis, and gel permeation chromatography in concert with light scattering (GPC-LS). Both adhesive polymers were cast into thin-films and their extent of swelling, *in vitro* degradation rate, and mechanical properties were characterized. Finally, methods for coating the adhesive polymer and the adhesive performance of the adhesive-coated biologic meshes were determined.

Materials

Polycaprolactone-diol MW1250 (PCL1250), polycaprolactone-diol MW2000 (PCL2000), polycaprolactone-triol MW900, succinic acid (SA), concentrated hydrochloric acid, *N*-Boc-Gly-OH, 3,4-dihydroxyhydrocinnamic acid (DOHA), 20% phosgene solution, dopamine hydrochloride, pyridine, and 4-dimethylaminopyridine (DMAP) were obtained from Sigma Aldrich (St. Louis, MO). *N*,*N*′-dicyclohexylcarbodiimide (DCC), 1-hydroxybenzotriazole hydrate (HOBt), and O-(benzotriazol-1-yl)-*N*,*N*,*N*′,*N*′-tetramethyluronium hexafluorophosphate (HBTU) were purchased from Chem-Impex International (Wood Dale,

IL), while dimethylformamide (DMF) was obtained from Acros (Fair Lawn, NJ). Chloroform, sodium chloride, magnesium sulfate, hexane, diethyl ether, trifluoroacetic acid, triethylamine, toluene, *N*-hydroxysuccinimide (NHS), and methanol were obtained from Fisher Scientific (Pittsburg, PA). 4ARM-PEG10K-NH_2-HCl and 4ARM-PEG10K-OH were purchased from Jenkem Technology USA, Inc. (Allen, TX). Bovine pericardium was obtained from Nirod Corporation (Ames, IA), while dialysis tubing (Spectrapor 7; 15,000 MWCO) was obtained from Spectrum Laboratories, Inc. (Rancho Dominquez, CA).

Synthesis of PCL1250-diSA

PCL1250-disuccinic acid (**PCL1250-diSA**) was prepared by reacting succinic anhydride with PCL1250-diol to yield a diacid-functionalized oligomeric precursor used in the synthesis of **AP1**. 10 g of PCL1250 (8 mmol), 8 g of SA (80 mmol), 6.4 mL of pyridine (80 mmol), and 100 mL of chloroform were refluxed with Argon purging overnight. After adding 100 mL of chloroform, the mixture was washed successively with 100 mL each of 12.1 mM HCl, saturated NaCl, and nanopure water. The organic layer was dried over magnesium sulfate, and then the volume of the mixture was reduced by half using rotary evaporation. After pouring the mixture into 800 mL of a 1:1 mixture of hexane and diethyl ether, the polymer was precipitated overnight at 4°C. The polymer was collected and dried under vacuum to yield 8.1 g of PCL1250-diSA. ^{1}H NMR (400 MHz, $CDCl_3$/TMS): δ 4.3 (s, 12H, -OOC-C*H*$_2$-$(CH_2)_4$-O-), 4.1 (s, 2H,C*H*$_2$-OOC-$(CH_2)_4CH_2$-O-), 3.6 (s, 4H, -*PEG*-), 2.7 (m, 4H,-OOCC*H*$_2$C*H*$_2$COOH), 2.3 (m, 12H, -OOC-$(CH_2)_4$- C*H*$_2$-O-), 1.5 (m, 24H, -OOC-CH_2-C*H*$_2$-CH_2- C*H*$_2$-CH_2-O-), 1.3 (m, 12H, -OOC-$(CH_2)_2$-C*H*$_2$-$(CH_2)_2$-O).

Synthesis of Adhesive Polymer 1 (AP1)

A solution of 0.338 g of HOBt (2.5 mmol), 0.950 g of HBTU (2.5 mmol), and 280 μL of triethylamine (2.0 mmol) in 20 mL of chloroform and 30 mL of DMF was added drop-wise over 60 min to a mixture of 4-arm PEG-Amine (5 g, 0.5 mmol), **PCL1250-diSA** (0.625 g, 0.5 mmol), DOHA (0.228 g, 1.25 mmol), and 20 mL of DMF. After the reaction mixture was stirred for 24 hours, 0.0455 g of DOHA (0.25 mmol) was added and the mixture was further stirred at room temperature for 1 hour. This solution was filtered into diethyl ether and precipitated overnight at 4°C. The precipitate was collected by vacuum filtration and dried under vacuum for 24 hours. The polymer was then dissolved with 75 mL each of 50 mM HCl and methanol, and dialyzed (15,000 MWCO) in 4 L of water (acidified to pH 3.5 with concentrated HCl) for 2 days. 3.8g of **AP1** was obtained after lyophilization. ^{1}H NMR (400 MHz, DMSO/TMS): δ 8.7-8.5 (s, 2H, -C_6H_3(O*H*)$_2$), 7.9 (d, 2H, -PEG-CON*H*CH2), 6.6-6.4 (dd, 3H, -C_6H_3(OH)$_2$), 4.1 (s, 2H, -PEG-O-CH_2-C*H*$_2$-NHCO-), 4.0 (t, 12H, -OOC-C*H*$_2$-$(CH_2)_4$-O-), 3.8-3.5 (m, 224H, -*PEG*-), 3.4 (s, 2H, -NHCOC*H*$_2$$CH_2$ $C_6H_3(OH)_2$ -), 3.3 (s, 4H, -PCL-*PEG*-PCL-), 3.2 (s, 2H, -NHCOCH_2C*H*$_2$ $C_6H_3(OH)_2$ -), 2.3 (m, 14H, -OOC-$(CH_2)_4$-C*H*$_2$-OOCCH2C*H*$_2$CONH-), 1.5 (m, 24H, -OOC-CH_2-C*H*$_2$-CH_2- C*H*$_2$-CH_2-O-), 1.3 (m, 12H, -OOC-(CH $_2)_2$-C*H*$_2$-$(CH_2)_2$-O). UV-vis: 3.6 ± 0.33 wt% DOHA. GPC-LS: Mw = 98,000; PD = 2.8.

Synthesis of PCL2000-diGly

Di-glycine functionalized PCL2000 (**PCL2000-diGly**) was synthesized by reacting PCL2000-diol with *N*-Boc-Gly-OH followed by Boc removal to yield a diamine oligomeric precursor used in the synthesis of **AP2**. 10 g of PCL2000 (5 mmol) and 2.63 g of Boc-Gly-OH (15 mmol) were dissolved with 60 mL chloroform, and purged with Argon for 30 minutes. 3.10 g of DCC (15 mmol) and 61.1 mg of DMAP (0.5 mmol) were then added to the reaction mixture, and the reaction was stirred overnight with Argon purging. The solution was filtered into 400 mL of diethyl ether. The precipitate was collected through filtration and dried under vacuum to yield 4.30 g of PCL2000-diBocGly. The Boc protecting

group was removed by reacting the polymer in 14.3 mL each of chloroform and trifluoroacetic acid for 30 minutes. After precipitation twice in diethyl ether, the polymer was dried under vacuum to yield 3.13 g of PCL2000-diGly. ^{1}H NMR (400 MHz, $CDCl_3$/TMS): δ 4.2 (m, 4H, -C*H*$_2$NH$_2$) 4.0 (t, 16H, -OOC-(CH$_2$)$_4$-C*H*$_2$-O-), 3.8-3.6 (t, 4H, -O-C*H*$_2$C*H*$_2$-O-), 2.3 (t, 16H, -OOC-C*H*$_2$(CH$_2$)$_4$-O-), 1.7 (m, 32H, -OOC-CH$_2$-C*H*$_2$-CH$_2$- C*H*$_2$-CH$_2$-O-), 1.3 (m, 16H, -OOC-(CH$_2$)$_2$-C*H*$_2$-(CH$_2$)$_2$-O-).

Synthesis of Adhesive Polymer 2 (AP2)

10 g of 4-arm PEG-OH (1 mmol) and 180 mL of toluene were placed in a 500 mL round-bottom flask equipped with a condenser and a Dean-Stark apparatus. While purging with Argon, the PEG was dried via azeotropic evaporation until 90 mL of toluene had been evaporated. After the mixture cooled to room temperature, 10.6 mL of 20% phosgene solution in toluene (20 mmol phosgene) was added, and the mixture was further stirred in a 50–60°C oil bath for 4 hours while purging with Argon. The toluene was then removed via rotary evaporation and further dried under vacuum overnight. Then, 691 mg of NHS (6 mmol) and 65 mL of chloroform were added to the dried polymer, and the mixture was stirred under Argon until the polymer dissolved. After drop-wise addition of 840 μl of triethylamine (6 mmol) in 10 mL of chloroform, the reaction mixture was stirred with Argon purging for 4 hours. Next, 427 mg of dopamine hydrochloride (2.2 mmol) in 25 mL of DMF and 307 μl of triethylamine (2.2 mmol) were added, and the mixture was stirred for 4 hours. Subsequently, 2.4 g of **PCL2000-diGly** (1 mmol) and 280 μL of triethylamine (2 mmol) were added, and the reaction mixture was stirred overnight. Then, 133 mg of dopamine hydrochloride (0.7 mmol) was added to cap the reaction along with 98 μl of triethylamine (0.7 mmol). The mixture was precipitated in diethyl ether, and the collected precipitate was dried under vacuum. The crude polymer was dissolved in 150 mL of methanol and 100 mL 50 mM HCl, and dialyzed (15,000 MWCO dialysis tubing) in 4 L of water at pH 3.5 for 2 days. Lyophilization yielded 3.3 g of **AP2.** ^{1}H NMR (400 MHz, DMSO/TMS): δ 8.7-8.5 (s, 2H, -C$_6$H$_3$(O*H*)$_2$), 7.6 (t, 1H,–PCL-OOC-CH$_2$-N*H*COO-CH$_2$-CH$_2$-O-), 7.2 (t, 1H, CH$_2$-CH$_2$-OOCN*H*-CH$_2$-CH$_2$-C$_6$H$_3$*(OH)$_2$*), 6.7-6.4 (d, 3H, -C$_6$*H*$_3$(OH)$_2$), 4.2 (m, 2H, -OOC-C*H*$_2$NHCOO-), 4.0 (m, 16H, -OOC-(CH$_2$)$_4$-C*H*$_2$-O-), 3.7-3.3 (m, PEG, -O-C*H*$_2$-C*H*$_2$-O-), 3.3-3.1 (m, 4H, CH$_2$-CH$_2$-NHCOO-C*H*$_2$-C*H*$_2$-C$_6$H$_3$*(OH)$_2$*), 2.3 (t, 16H, -OOC-C*H*$_2$(CH$_2$)$_4$-O-), 1.7 (m, 32H, -OOC-CH$_2$-C*H*$_2$-CH$_2$- C*H*$_2$-CH$_2$-O-), 1.3 (m, 16H, -OOC-(CH$_2$)$_2$-C*H*$_2$-(CH$_2$)$_2$-O-). UV-vis: 2.92 ± 0.34 wt% dopamine. GPC-LS: Mw = 66,000; PD = 4.4.

Characterization of adhesive polymer

^{1}H NMR was performed at the National Magnetic Resonance Facility at Madison (NMRFAM) located at the University of Wisconsin-Madison for the purpose of determining the composition of the adhesive polymers (i.e., PEG and PCL content). The catechol content of the block copolymers was determined using UV absorbance of polymer solutions in methanol or DMSO at the maximum absorbance wavelength of the catechol (λ_{max} = 280 nm). Solutions containing known concentrations of DOHA or dopamine were used to construct the calibration curve.

Molecular weight of polymers was determined by GPC-LS on an Optilab® rEX (Wyatt Technology) refractive index detector and a miniDAWN™ TREOS (Wyatt Technology) triple-angle light scattering detector using Shodex-OH Pak columns (SB-804 HQ and SB-802.5 HQ). Either 50:50 mixture of methanol and phosphate buffered saline (**AP1**) or DMF (**AP2**) was used as the mobile phase. The experimentally determined reflective index (dn/dc) value of each polymer was used for the molecular weight calculation.

Characterization of polymer film

Adhesive polymers were cast into films from solutions of either methanol or chloroform, and their percent swelling, *in vitro* degradation profiles, and tensile mechanical properties were determined. For each test, the films were cured by the addition of a sodium periodate ($NaIO_4$) solution which promotes oxidative crosslinking of the catechol. Additionally, up to 30 wt% of PCL-triol was formulated into the adhesive films to determine the effect of added PCL content on the physical and mechanical properties of the adhesives. The equilibrium swelling of the adhesive films in phosphate buffered saline (PBS, pH 7.4, 37°C, 24 hours) was calculated by the equation, W_s/W_d, where W_d and W_s are the weights of the dry and swollen films, respectively. *In vitro* degradation was determined by monitoring the mass loss of the adhesive films incubated in PBS (pH 7.4) over time at 37°C.

For tensile mechanical testing, adhesive films were cast in a dog-bone shaped mold (9.53 mm gauge length, 3.80 mm gauge width, and 12.7 mm fillet radius) and swollen in PBS (pH 7.4) for 1 hour prior to testing. Films were loaded to failure at a rate of 10 mm/min using a materials test machine (Admet, Inc., Norwood, MA). The maximum tensile strength and failure strain were recorded. Stress vs. strain curves were also used to calculate the Young's modulus (initial slope) and toughness (area under the curve).

Coating adhesive film onto biologic mesh

Polymer solutions were solvent cast (methanol or chloroform) over the biologic meshes, and then dried under vacuum overnight. In order to control the thickness of the films, the polymers were casted at coating densities of 15–90 g/m^2. The thickness of the coatings was determined by measuring the difference between the average thicknesses of coated and uncoated meshes (n=6) using a digital micrometer (Fred V. Fowler Company, Newton, MA). Similarly, the mass of the coated films was determined by the difference between the average masses of the coated and uncoated meshes (n=6).

Method for adhesion testing

Adhesive properties of the coated meshes were determined using lap shear and burst strength adhesion tests (Figure 2) in accordance with American Society for Testing and Materials (ASTM) standards. For the lap shear test (ASTM F2255),[40] adhesive-coated mesh segments were cut into 2.5 cm × 5 cm strips, hydrated in PBS, and then activated by addition of a solution of $NaIO_4$ (40 μL) prior to bringing the coated mesh into contact (2.5 cm × 1 cm overlap) with the test substrate (bovine pericardium; 2.5 cm × 5 cm). The adhesive joint was compressed with a 100 g weight for 2 hours, and further conditioned in PBS (37°C) for another hour prior to testing. The adhesive joints were loaded to failure in shear at a rate of 10 mm/min, and the maximum strength and failure strain were recorded. Additionally, the work of adhesion was determined by the area under the strength vs. strain curve and normalized by the initial contact area of the adhesive joint. Lap shear test conditions included assessing the effect of varying $NaIO_4$ concentrations, polymer coating density, and PCL-triol addition.

For the burst adhesion test (ASTM F2392),[41] the adhesive-coated mesh segments were cut into 15 mm-diameter circular samples and conditioned in the same manner as with the lap shear testing. A 40 mm-diameter circular piece of bovine pericardium with a concentric 3 mm-diameter defect served as the test substrate. A syringe pump was used to push PBS against the adhesive joint until the solution burst through the seal, and the burst pressure was recorded.

For both tests, sample size was 6. Commercially available tissue adhesives such as cyanoacrylate (Dermabond®, Ethicon Inc.) and fibrin glue (Tisseel™, Baxter Healthcare

Corporation) were utilized for comparison purposes. These adhesives were applied *in situ* onto bovine pericardium substrates according to the instructions of the manufacturer.

Statistical analysis

Statistical analysis was performed using an analysis of variance (ANOVA) and Tukey post hoc analysis with a significance level of $p = 0.05$.

3 Results and Discussion

Synthesis of new adhesive polymers

Two new adhesive polymers (**AP1** and **AP2**) were synthesized according to Schemes 1 and 2, respectively, and their chemical compositions are shown in Table 1. These adhesive polymers are amphiphilic multiblock copolymers constructed from a hydrophilic 4-armed PEG and a linear bifunctional, hydrophobic polyester, PCL. The presence of PEG allows the adhesive polymer to remain relatively hydrophilic in order to achieve good “wetting” or adhesive contact with both the biologic mesh and the tissue substrate. The branched architecture of PEG was utilized both for chain extension of the polymer backbone through reacting with bifunctional PCL, as well as coupling with adhesive molecules, 3,4-dihydroxyhydrocinnamic acid (DOHA) or dopamine, through a one-step synthesis. **AP1** was synthesized by coupling terminal amine groups of 4-armed PEG-amine with the carboxyl termini of **PCL1250-diSA** to form amide linkages using carbodiimide chemistry. In the synthesis of **AP2**, 4-arm PEG-OH (activated with phosgene and then NHS) was reacted with terminal amine groups of **PCL2000-diGly** to form urethane linkages. **AP2**, which utilized a higher molecular weight PCL in the synthesis, has a higher PCL content (20.6 wt%) as compared to **AP1** (13.4 wt%). The catechol contents for both adhesive polymers are approximately 3 wt%. These adhesive molecules are responsible for interfacial binding as well as further solidifying the adhesive film when an oxidant is introduced. Catechols are converted to highly reactive quinones which can result in covalent crosslinking with other catechols within the adhesive film (cohesive crosslinking),[42] or with functional groups such as amine and thiol found on tissue surfaces (adhesive crosslinking). [30, 43]

Characterization of adhesive polymer films

The degree of swelling was affected by the composition of the adhesive formulation, as well as the coating density (mass of polymer per unit area) of the films (Table 2). For example, higher PCL content in **AP2** resulted in less swelling compared to **AP1**. When PCL-triol was added to both polymers, these formulations exhibited significantly less swelling. These observations were expected since the extent of water uptake is related to the hydrophobicity of the films. In addition to PCL content, the polymer coating density also affected the extent of swelling, with films formed with half the coating density absorbing 1.4 times more water. The coating density likely affected the crosslinking density of the film, which is known to be inversely proportional to the degree of swelling. [42]

The mechanical properties of the film were also found to be strongly affected by the PCL content (Table 3). For example, **AP2** demonstrated significantly higher tensile strength and toughness, compared to **AP1**. Strength and toughness values for **AP2** formulated with the addition of 30 wt% of PCL-triol were even greater, suggesting that the mechanical properties of these adhesives can be modulated by blending them with compounds that impart the desired characteristics. Note that the toughness more than doubled with the addition of PCL-triol to **AP2**. The addition of PCL-triol increased the crosslinking density in the film, which resulted in the observed increase in mechanical properties. This increase in crosslinking density did not result in brittle films as reflected in the elevated strain to failure values.

The more hydrophilic **AP1** films degraded at a faster rate as compared to **AP2** (Figure 3). Since our adhesive films degrade mainly through hydrolysis of ester linkages within the PCL blocks, the greater water uptake by **AP1** (correlated with elevated swelling) resulted in faster degradation. However, when 30 wt% PCL-triol (MW = 900) was blended into the polymer film, the degradation rate increased. Although PCL-triol increased the overall hydrophobicity of the film, the faster rate of mass loss may be due to the rapid release of the lower molecular weight oligomers through diffusion. Apart from film hydrophobicity, pH of surrounding media may play a role in the rate of degradation. The rate of hydrolysis can be reduced in slightly more acidic pH or increased when the film was incubated in a more basic solution (data not shown). However, we did not observe significant change in the pH of the PBS buffer over the course of the study.

These results demonstrate that both the chemical architecture and adhesive formulation play a significant role in the physical and mechanical properties of the adhesive films. Specifically, the hydrophobicity of the film had a significant impact on the extent of swelling, which was found to be related in an inverse manner to the mechanical properties and rate of hydrolysis. These observations are in agreement with amphiphilic multiblock copolymer films reported in the literature. [44–47] By designing the adhesive polymers with different compositions, we were able to tailor these properties, which were further refined by blending these polymers with PCL-triol.

Adhesive coated on bovine pericardium

Bovine pericardium was first evaluated as backing material for the adhesive coating. This biomaterial was chosen because it is an inexpensive and readily abundant extracellular matrix with suitable mechanical properties (tensile failure load of 41 ± 9.8 N/cm). Additionally, several acellular bovine pericardium-based products (e.g., Veritas®, Synovis Surgical Innovations; Tutomesh®, RTI Biologics) have been approved by the FDA for soft tissue reconstruction.[48–50]

Adhesive performance of the coated bovine pericardium was evaluated using lap shear and burst strength adhesion tests. Both lap shear strength and work of adhesion, the total amount of energy required to separate the adhesive joint, increased with increasing $NaIO_4$ concentration, but exhibited no further increase when the concentration exceeded 20 mg/mL (Table 4). To minimize potential *in vivo* complications with using this oxidant, the lowest possible amount (20 mg/mL) was used in subsequent testing whenever possible. Varying the polymer coating density also affected the adhesive properties (Table 5), with higher coating densities yielding higher adhesive strengths for both lap shear and burst tests. The adhesive-mesh constructs were created using a loading density of at least 60 g/m^2 in subsequent testing. When **AP1** was formulated with PCL-triol (Table 6), no change in adhesive strengths was observed. However, the work of adhesion was significantly increased at the highest PCL-triol (30 wt%) content tested.

Using the optimized parameters (20 mg/mL $NaIO_4$ and coating density of 60 g/m^2) from the previous adhesion tests, the adhesive properties of the bioadhesive constructs were determined and compared to commercially available bioadhesives: Dermabond® (a cyanoacrylate adhesive) and Tisseel™ (a fibrin adhesive). While Dermabond exhibited the highest adhesive strengths for both lap shear and burst strength adhesion tests (Figures 4 and 5, respectively), the adhesive-coated pericardium significantly outperformed Tisseel. For example, **AP1** (70.0 ± 9.50 kPa) and **AP2** (107 ± 24.7 kPa) demonstrated adhesive strengths that were 27 and 42 times higher than that of Tisseel (2.58 ± 1.76 kPa). Given that the adhesive performances of **AP1** and **AP2** were statistically equivalent, **AP1** was used in subsequent testing.

Adhesive film coated on commercial biologic mesh

Three commercially available biologic hernia meshes derived from multilayered porcine small intestinal submucosa (Surgisis®, Cook Biotech) and crosslinked porcine dermal tissue (Permacol™, Covidien, and CollaMend®, C.R. Bard) were coated with **AP1.** Regardless of the mesh type, **AP1** outperformed Tisseel by more than ten-fold (Figure 6). While the **AP1** constructs only exhibited adhesive strengths that were 30–60% of those of Dermabond, it is possible to further optimize the coating technique or adhesive formulation specific to each mesh type. As shown in Table 7, the measured coating mass on each mesh type was nearly equivalent as they were coated with the same coating density (90 g/m^2). However, the measured coating thicknesses on both the Permacol and Surgisis meshes were significantly less than that on CollaMend. It is likely that when the polymer solution was directly applied onto these meshes, the solution soaked into the porous matrices and the lower coating thicknesses may have contributed to the lower adhesive strength values.

Exploiting nature's adhesive molecule

A new series of synthetic biomimetic adhesives that combines the superior mechanical properties of amphiphilic multiblock copolymers with water-resistant adhesive moieties is described. These polymers are either functionalized with DOHA or dopamine (Figure 7), which resemble the catecholic side chain of DOPA that marine mussels utilize to form strong bonds in the presence of water. We exploited catechol's ability to crosslink with both the biologic mesh and tissue substrate to generate strong interfacial bonds. The adhesive property of the phenylic functional group is triggered by the addition of oxidant ($NaIO_4$) that converts the catechol to highly reactive quinone, which has been shown to be critical for binding to soft tissue surfaces.[30] While $NaIO_4$ is an irritant and strong oxidant, it is reduced to benign iodide through the red-ox reaction with catechol. Additionally, a $NaIO_4$-cured PEG-DOHA sealant was demonstrated to be non-toxic [22] and elicited minimal inflammatory responses *in vivo*,[51] indicating that the use of $NaIO_4$ appears to be a potentially viable method for activating these biomimetic adhesives.

PEG-catechol conjugates have been previously studied as potential tissue adhesives. [33], [42], [51] However, relatively fragile PEG hydrogels were used as the bulk supporting material for these adhesives, and the associated mechanical properties were significantly lower than those for the adhesives in this report. While the tensile strength of PEG-based hydrogels can increase with increasing cross-linking density, densely cross-linked hydrogels are also brittle and fracture at relatively low strain.[52] To improve the adhesive performance of DOPA-based adhesives, we combined nature's water-resistant adhesive molecules with amphiphilic multiblock copolymer films, which are known to have excellent mechanical properties even when swollen.[44–47] Unlike hydrophilic PEG-based hydrogels, which can swell excessively and become fragile, hydrophobic PCL content was used to control the swelling of the proposed films, which in turn, modulated the cohesive properties of the films. Even with elevated PCL content, these adhesive films demonstrated elevated mechanical properties while still retaining relatively high failure strain. These PCL segments readily self-assemble in an aqueous environment through hydrophobic-hydrophobic interaction to form cross-linking points, which is a likely source of the elevated mechanical properties.

The adhesive performances of the adhesive-coated constructs are strongly affected by the bulk mechanical properties of the films. For example, formulations that yielded films with reduced swelling or high tensile properties (i.e. elevated PCL content, increased coating densities) also resulted in elevated adhesive properties. This observation is in agreement with literature findings where it was reported that films with elevated mechanical properties correlated to high lap shear adhesion strength.[53] Additionally, degradation profiles of these adhesives can be tailored by both the composition of the polymer as well as the

incorporation of PCL-triol. Our ability to control various properties of the adhesive in a predictable manner can be used to tailor the adhesive formulation to match the specification of a given application.

Potential clinical implications

The use of tissue adhesives is a relatively new approach in mesh fixation that can potentially alleviate the debilitating side effects associated with currently used perforating fixation devices (sutures, tacks, and staples). Specifically, mesh fixation has been linked to postoperative pain in as many as 63% of hernia repair procedures, with pain that alters patients' quality of life occurring in 4–12% of the cases.[9, 11] Postoperative evaluation that compared mesh fixation with staples versus fibrin glue found that the prevalence of chronic pain was significantly higher in the stapled group (21%) than in the fibrin sealant group (4.7%).[16] In some instances, however, fibrin glue alone cannot effectively secure meshes *in vivo* due to its poor adhesive strength,[14, 15] while stronger bioadhesives such as cyanoacrylate and GRF have inherently undesirable characteristics (i.e., toxic degradation products and poor biomechanical properties).[18, 19] Further, existing tissue adhesives require preparation prior to use, which may complicate surgical work flow.

The bioadhesive constructs described herein demonstrated burst pressures that are well above reported physiological intra-abdominal pressures (64–252 mm Hg),[54] and significantly outperformed fibrin-based adhesives which have been reported to have some level of success in hernia mesh fixation *in vivo*.[15–17] A pre-coated adhesive mesh that binds strongly to tissue and degrades over time when its function is no longer required can potentially eliminate the need for mechanical fixation methods while improving long-term patient comfort.

4 Conclusion

In this paper, we combined a novel polymer design, a biomimetic approach, and biofunctional materials to address a substantial clinical shortcoming. Two new adhesive polymers were synthesized and coated onto several biologic meshes. These adhesive-coated constructs demonstrated significantly higher adhesive strength as compared to fibrin glue. The adhesive properties and rate of degradation, as well as the physical and mechanical properties of the adhesive films can be tailored based on polymer composition, coating density, oxidant concentration, and PCL-triol content. The coating process can be applied to different commercial biologic meshes ranging from cross-linked dermal tissues to multilayered porcine small intestine submucosa, while imparting strong water-resistant adhesive properties to these scaffolds. Based on lap shear and burst strength adhesion tests, these bioadhesive constructs demonstrated adhesive properties that may be suitable for soft tissue reconstruction.

Acknowledgments

This work was supported by NIH (1R43DK083199-01). NMR was performed at the NMRFAM, which is supported by NIH (P41RR02301 P41GM66326, P41GM66326, P41RR02301, RR02781, RR08438), NSF (DMB-8415048, OIA-9977486, BIR-9214394), University of Wisconsin, and U.S. Department of Agriculture. The authors gratefully acknowledge Dr. Yuri W. Novitsky (Connecticut Comprehensive Center for Hernia Repair at the University of Connecticut) for providing clinically relevant discussions.

References

1. Ansaloni L, Catena F, Gagliardi S, Gazzotti F, D'Alessandro L, Pinna AD. Hernia repair with porcine small-intestinal submucosa. Hernia. 2007; 11 (4):321–326. [PubMed: 17443270]

2. Catena F, Ansaloni L, Gazzotti F, Gagliardi S, Di Saverio S, D'Alessandro L, Pinna AD. Use of porcine dermal collagen graft (Permacol) for hernia repair in contaminated fields. Hernia. 2007; 11:57–60. [PubMed: 17119853]

3. Franklin MEJ, Gonzalez JJ Jr, Glass JL. Use of porcine small intestinal submucosa as a prosthetic device for laparoscopic repair of hernias in contaminated fields: 2 year follow-up. Hernia. 2004; 8:186–189. [PubMed: 14991410]

4. Lee DK. Achilles tendon repair with acellular tissue graft augmentation in neglected ruptures. J Foot Ankle Surg. 2007; 46 (6):451–5. [PubMed: 17980842]

5. Bond JL, Dopirak RM, Higgins J, Burns J, Snyder SJ. Arthroscopic replacement of massive, irreparable rotator cuff tears using a GraftJacket allograft: technique and preliminary results. Arthroscopy. 2008; 24 (4):403–409. [PubMed: 18375271]

6. Santibáñez-Salgado JA, Olmos-Zúñiga JR, Pérez-López M, Aboitiz-Rivera C, Gaxiola-Gaxiola M, Jasso-Victoria R, Sotres-Vega A, Baltazares-Lipp M, Pérez-Covarrubias D, JVC. Lyophilized glutaraldehyde-preserved bovine pericardium for experimental atrial septal defect closure. Eur Cell Mater. 2010; 19:158–65. [PubMed: 20408127]

7. Narotam PK, Reddy K, Fewer D, Qiao F, Nathoo N. Collagen matrix duraplasty for cranial and spinal surgery: a clinical and imaging study. J Neurosurg. 2007; 106 (1):45–51. [PubMed: 17236486]

8. Hidalgo M, Castillo MJ, Eymar JL, Hidalgo A. Lichtenstein inguinal hernioplasty: sutures versus glue. Hernia. 2005; 9 (3):242–244. [PubMed: 15891811]

9. Koniger J, Redecke J, Butters M. Chronic pain after hernia repair: a randomized trial comparing Shouldice, Lichtenstein and TAPP. Langenbecks Arch Surg. 2004; 389:361–365. [PubMed: 15243743]

10. Stark E, Oestreich K, Wendl K, Rumstadt B, Hagmüller E. Nerve irritation after laparoscopic hernia repair. Surg Endosc. 1999; 13 (9):878–81. [PubMed: 10449843]

11. Berndsen FH, Petersson U, Arvidsson D, Leijonmarck CE, Rudberg C, Smedberg S, Montgomery A. Discomfort five years after laparoscopic and Shouldice inguinal hernia repair: a randomised trial with 867 patients. Hernia. 2008; 12 (4):445–446. [PubMed: 18270787]

12. Barber FA, Herbert MA, Boothby MH. Ultimate tensile failure loads of a human dermal allograft rotator cuff augmentation. Arthroscopy. 2008; 24 (1):20–24. [PubMed: 18182197]

13. Barber FA, Herbert MA, Coons DA. Tendon augmentation grafts: biomechanical failure loads and failure patterns. Arthroscopy. 2006; 22 (5):534–538. [PubMed: 16651164]

14. Eriksen JR, Bech JI, Linnemann D, Rosenberg J. Laparoscopic intraperitoneal mesh fixation with fibrin sealant (Tisseel) vs. titanium tacks: a randomised controlled experimental study in pigs. Hernia. 2008; 12:483–491. [PubMed: 18483783]

15. Olivier ten Hallers EJ, Jansen JA, Marres HAM, Rakhorst G, Verkerke GJ. Histological assessment of titanium and polypropylene fiber mesh implantation with and without fibrin tissue glue. Journal of Biomedical Materials Research Part A. 2006:372–380. [PubMed: 16673390]

16. Schwab R, Willms A, Kroger A, Becker HP. Less chronic pain following mesh fixation using fibrin sealant in TEP inguinal hernia repair. Hernia. 2006; 10:272–277. [PubMed: 16554980]

17. Topart P, Vandenbroucke F, Lozac'h P. Tisseel vs tack staples as mesh fixation in totally extraperitoneal laparoscopic repair of groin hernias. Surg Endosc. 2005; 19:724–727. [PubMed: 15759187]

18. Fortelny RH, Petter-Puchner AH, Walder N, Mittermayr R, Öhlinger W, Heinze A, Redl H. Cyanoacrylate tissue sealant impairs tissue integration of macroporous mesh in experimental hernia repair. Surgical Endoscopy. 2007; 21 (10):1781–1785. [PubMed: 17356940]

19. Jain SK, Vindal A. Gelatin–resorcin–formalin (GRF) tissue glue as a novel technique for fixing prosthetic mesh in open hernia repair. Hernia. 2009; 13 (3):299–304. [PubMed: 19225855]

20. Sierra, D.; Saltz, R. Surgical Adhesives and Sealants: Current Technology and Applications. Technomic Publishing Company, Inc; Lancaster, PA: 1996.

21. Ikada, Y. Tissue adhesives. In: Chu, CC.; von Fraunhofer, JA.; Greisler, HP., editors. Wound Closure Biomaterials and Devices. CRC Press, Inc; Boca Raton, Florida: 1997. p. 317-346.

22. Bilic G, Brubaker C, Messersmith PB, Mallik AS, Quinn T, Done E, Gucciardo L, Zeisberger SM, Zimmermann R, Deprest J, Zisch AH. Injectible candidate sealants for fetal membrane repair:

Bonding and toxicity in vitro. American Journal of Obstetrics and Gynecology. 2010; 202 (85):1–9. [PubMed: 20096251]

23. Waite JH. Nature's underwater adhesive specialist. Int J Adhes Adhes. 1987; 7 (1):9–14.
24. Yamamoto H. Marine adhesive proteins and some biotechnological applications. Biotechnology and Genetic Engineering Reviews. 1996; 13:133–65. [PubMed: 8948111]
25. Kramer KJ, Morgan TD, Hopkins TL, Christensen A, Schaefer J. Insect cuticle tanning: Enzymes and cross-link structure. Natural Occurring Pest Bioregulators. 1991; 449:87–105.
26. Yu M, Hwang J, Deming TJ. Role of L-3,4-dihydroxyphenylanine in mussel adhesive proteins. Journal of American Chemical Society. 1999; 121 (24):5825–5826.
27. Deming TJ, Yu M, Hwang J. Mechanical studies of adhesion and crosslinkning in marine adhesive protein analogs. Polymeric Materials: Science and Engineering. 1999; 80:471–472.
28. Waite JH. Mussel beards: A coming of Age. Chemistry and Industry. 1991 Sep 2.:607–611.
29. Lee BP, Chao CY, Nunalee FN, Shull KR, Messersmith PB. Rapid Photocurable of Amphiphilic Block Copolymers Hydrogels with High DOPA Contents. Maclomolecules. 2006; 39:1740–48.
30. Guvendiren M, Messersmith PB, Shull KR. Self-Assembly and Adhesion of DOPA-Modified Methacrylic Triblock Hydrogels. Biomacromolecules. 2008; 9 (1):122–128. [PubMed: 18047285]
31. Huang K, Lee BP, Ingram D, Messersmith PB. Synthesis and Characterization of Self-Assembling Block Copolymers Containing Bioadhesive End Groups. Biomacromolecules. 2002; 3 (2):397–406. [PubMed: 11888328]
32. Catron ND, Lee H, Messersmith PB. Enhancement of poly(ethylene glycol) mucoadsorption by biomimetic end group functionalization. Biointerphases. 2006; 1 (4):134–141. [PubMed: 20408626]
33. Burke SA, Ritter-Jones M, Lee BP, Messersmith PB. Thermal gelation and tissue adhesion of biomimetic hydrogels. Biomed Mater. 2007; 2:203–210. [PubMed: 18458476]
34. Lee, BP. Biomimetic compounds and synthetic methods therefor. US Patent. 7,622,533. issued in 2009
35. Shao H, Bachus KN, Stewart RJ. A Water-Borne Adhesive Modeled after the Sandcastle Glue of P. californica. Macromolecular Biosciences. 2009; 9 (5):464–471.
36. Rauth TP, Poulose BK, Nanney LB, Holzman MD. A Comparative Analysis of Expanded Polytetrafluoroethylene and Small Intestinal Submucosa -- Implications for Patch Repair in Ventral Herniorrhaphy. Journal of Surgical Research. 2007; 143 (1):43–49. [PubMed: 17950071]
37. Lantis JCJ, Gallivan EK, Hekier R, Connolly R, Schwaitzberg SD. A comparison of collagen and PTFE patch repair in a rabbit model of congenital diaphragmatic hernia. Journal of Investigative Surgery. 2000; 13:319–325. [PubMed: 11202008]
38. Konstantinovic ML, Lagae P, Zheng F, Verbeken EK, De Ridder D, Deprest JA. Comparison of host response to polypropylene and non-cross-linked porcine small intestine serosal-derived collagen implants in a rat model. BJOG: an International Journal of Obstetrics and Gynecology. 2005; 112:1554–1560.
39. Gaertner WB, Bonsack ME, Delaney JP. Experimental Evaluation of Four Biologic Prostheses for Ventral Hernia Repair. Journal of Gastrointestinal Surgery. 2007; 11:1275–1285. [PubMed: 17674112]
40. ASTM-F2255. Standard Test Method for Strength Properties of Tissue Adhesives in Lap-Shear by Tension Loading. 2003.
41. ASTM-F2392. Standard Test Method for Burst Strength of Surgical Sealants. 2004.
42. Lee BP, Dalsin JL, Messersmith PB. Synthesis and Gelation of DOPA-Modified Poly(ethylene glycol) Hydrogels. Biomacromolecules. 2002; 3 (5):1038–47. [PubMed: 12217051]
43. Lee H, Scherer NF, Messersmith PB. Single Molecule Mechanics of Mussel Adhesion. Proc Natl Acad Sci. 2006; 103:12999–13003. [PubMed: 16920796]
44. Cohn D, Stern T, Gonzalez MF, Epstein J. Biodegradable poly(ethylene oxide)/poly(e-caprolactone) multiblock copolymers. Journal of Biomedical Materials Research. 2002; 59 (2): 273–281. [PubMed: 11745563]

45. Bae YH, Huh KM, Kim Y, Park K. Biodegradable amphiphilic multiblock copolymers and their implications for biomedical applications. Journal of Controlled Release. 2000; 64 (1–3):3–13. [PubMed: 10640641]

46. Nagata M, Kitazima I. Photocurable biodegradable poly(epsilon-caprolactone)/poly(ethylene glycol) multiblock copolymers showing shape-memory properties. Colloid & Polymer Science. 2006; 284:380–386.

47. Loh XJ, Sng KBC, Li J. Synthesis and water-swelling of thermo-responsive poly(ester urethane)s containing poly(caprolactone), poly(ethylene glycol) and poly(propylene glycol). Biomaterials. 2008; 29:3185–3194. [PubMed: 18456319]

48. Santillan-Doherty P, Jasso-Victoria R, Sotres-Vega A, Olmos R, Arreola JL, Garcia D, Vanda B, Gaxiola M, Santibanez A, Martin S, Cabello R. Thoracoabdominal wall repair with glutaraldehyde-preserved bovine pericardium. Journal of investigative surgery: the official journal of the Academy of Surgical Research. 1996; 9 (1):45–55. [PubMed: 8688380]

49. Burger JWA, Halm JA, Wijsmuller AR, ten Raa S, Jeekel J. Evaluation of new prosthetic meshes for ventral hernia repair. Surgical endoscopy. 2006; 20 (8):1320–5. [PubMed: 16865616]

50. Lo Menzo E, Martinez JM, Spector SA, Iglesias A, Degennaro V, Cappellani A. Use of biologic mesh for a complicated paracolostomy hernia. American journal of surgery. 2008; 196 (5):715–9. [PubMed: 18954603]

51. Brubaker CE, Kissler H, Wang LJ, Kaufman DB, Messersmith PB. Biological performance of mussel-inspired adhesive in extrahepatic islet transplantation. Biomaterials. 2010; 31:420–427. [PubMed: 19811819]

52. Temenoff JS, Athanasiou KA, LeBaron RG, Mikos AG. Effect of poly(ethylene glycol) molecular weight on tensile and swelling properties of oligo(poly(ethylene glycol) fumarate) hydrogels for cartilage tissue engineering. Journal of biomedical materials research. 2002; 59 (3):429–37. [PubMed: 11774300]

53. da Silva LFM, Rodrigues TNSS, Figueiredo MAV, de Moura MFSF, Chousal JAG. Effect of adhesive type and thickness on the lap shear strength. Journal of Adhesion. 2006; 82:1091–1115.

54. Cobb WS, Burns JM, Kercher KW, Matthews BD, James NH, Todd HB. Normal intraabdominal pressure in healthy adults. The Journal of Surgical Research. 2005; 129 (2):231–5. [PubMed: 16140336]

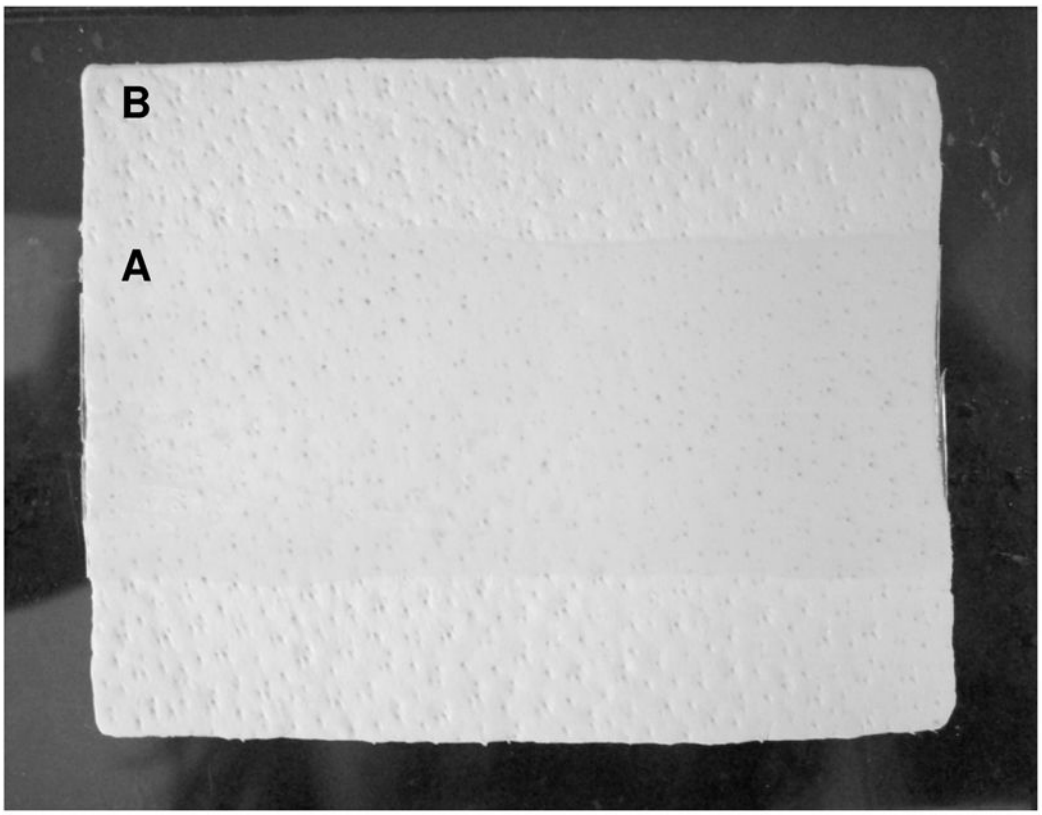

Figure 1.
Photograph of adhesive film (3cm×8cm) coated on a 6cm×8cm biologic mesh. **A** and **B** indicate adhesive-coated and uncoated regions, respectively.

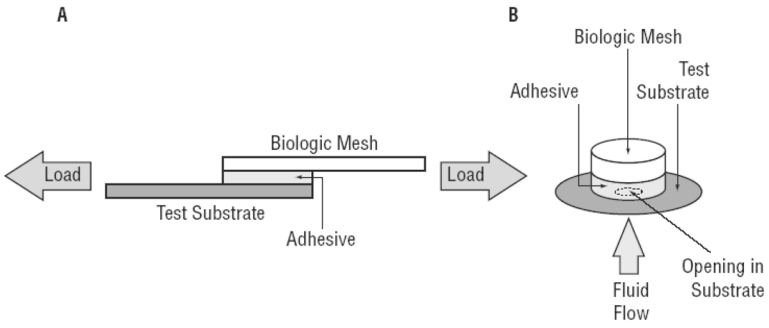

Figure 2.
Schematics of the setup for **A**) lap shear and **B**) burst strength tests.

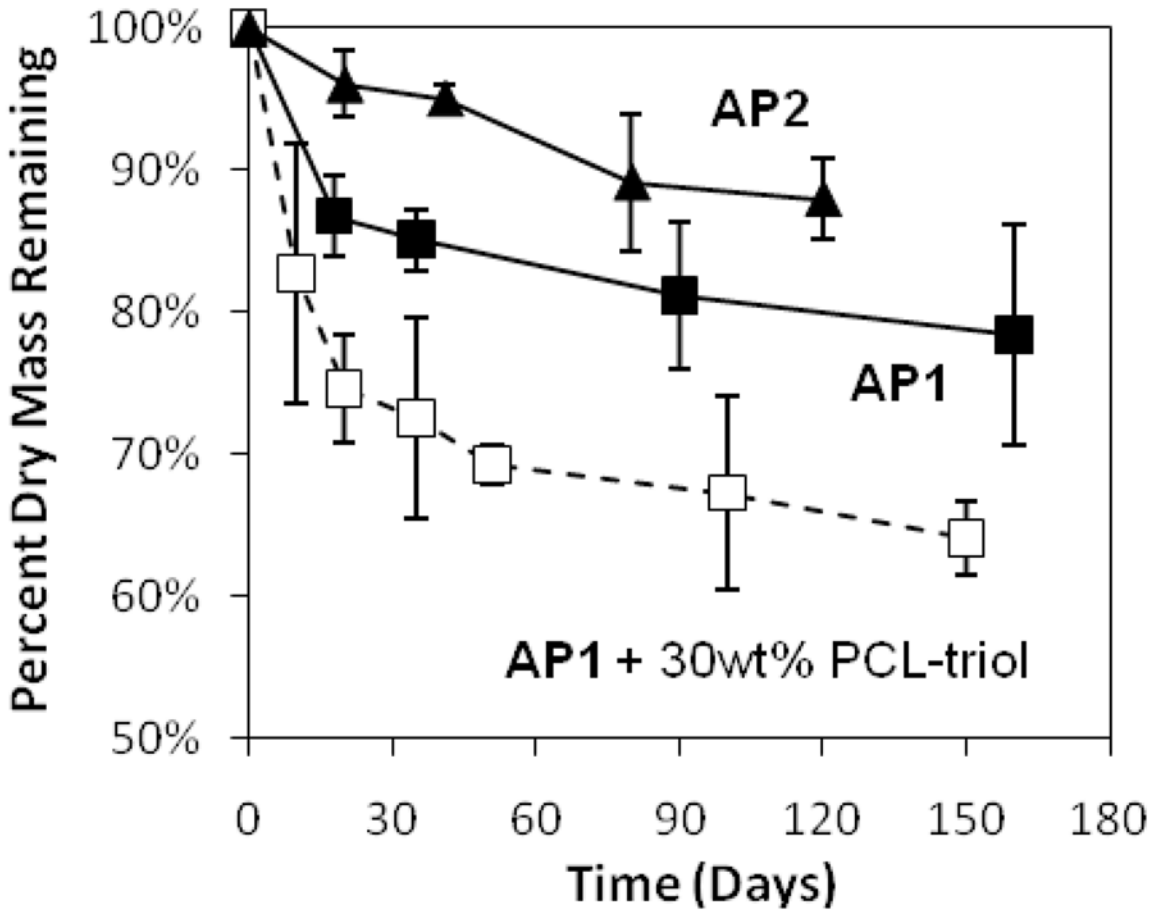

Figure 3.
In vitro degradation profile of adhesive films incubated at 37°C in PBS (pH 7.4).

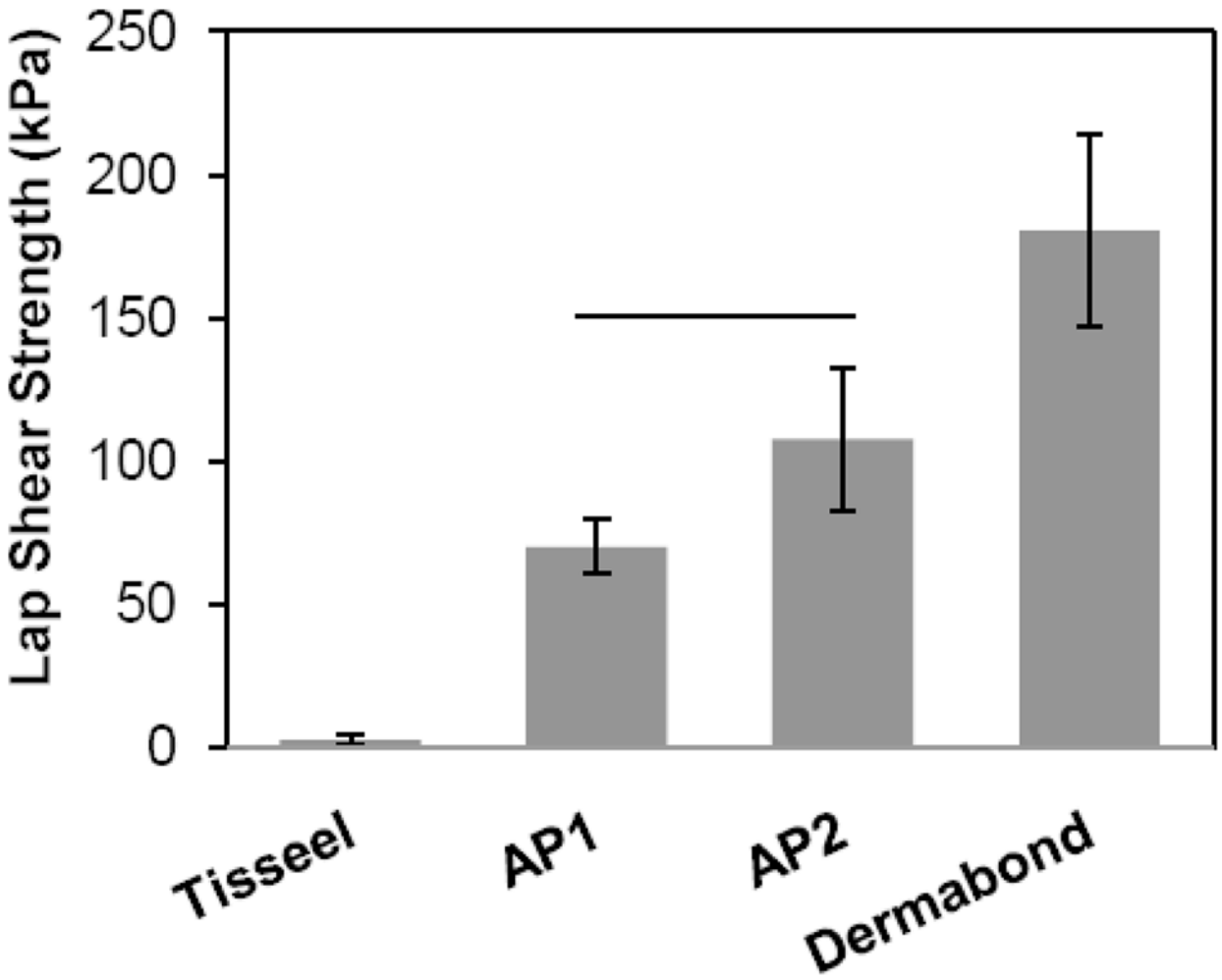

Figure 4.
Maximum adhesive shear strength for adhesive joints formed using adhesive-coated bovine pericardium. Solid line represents statistical equivalence ($p > 0.05$).

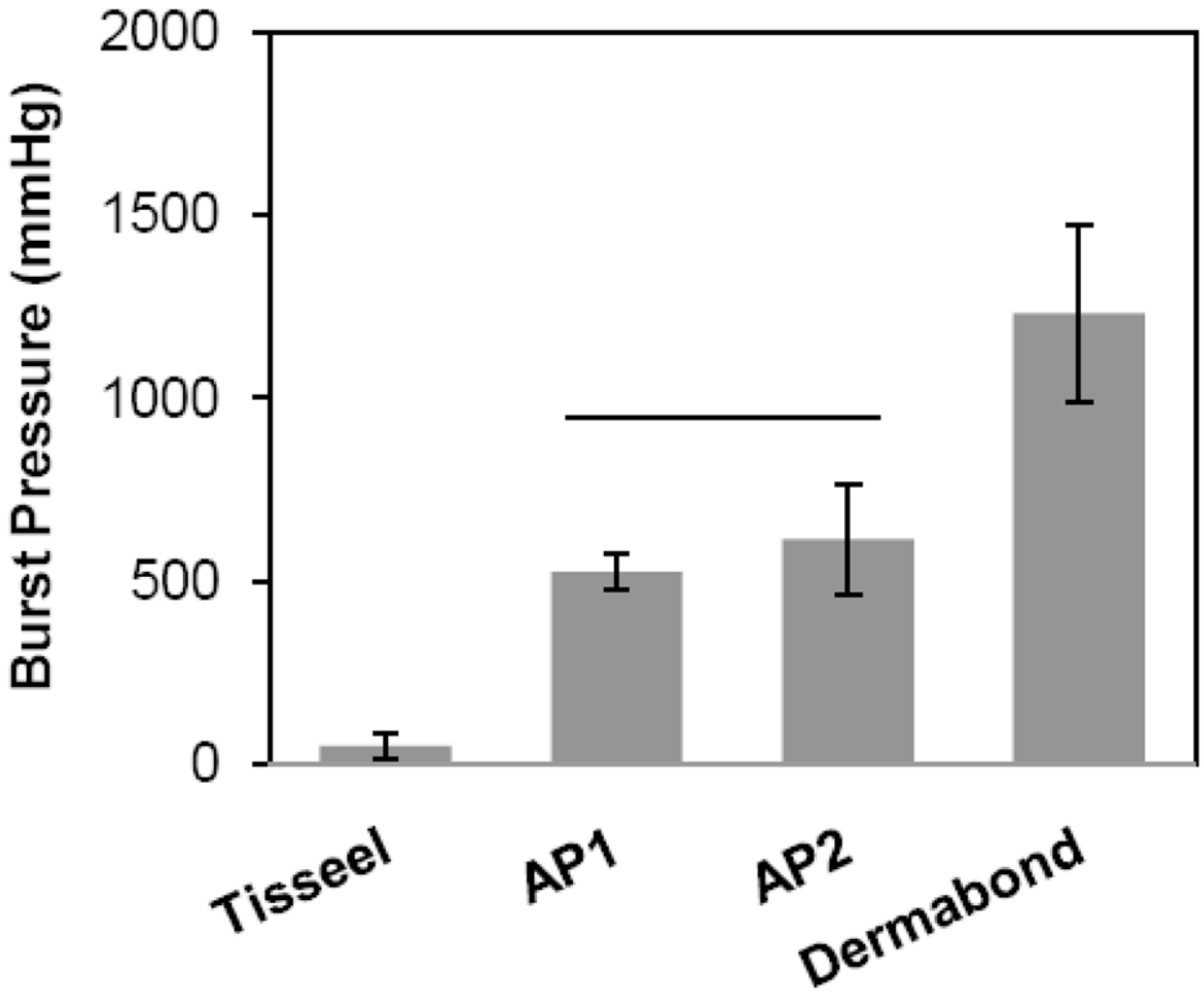

Figure 5.
Burst pressure of adhesive joints sealed with adhesive-coated bovine pericardium. Solid line represents statistical equivalence ($p > 0.05$).

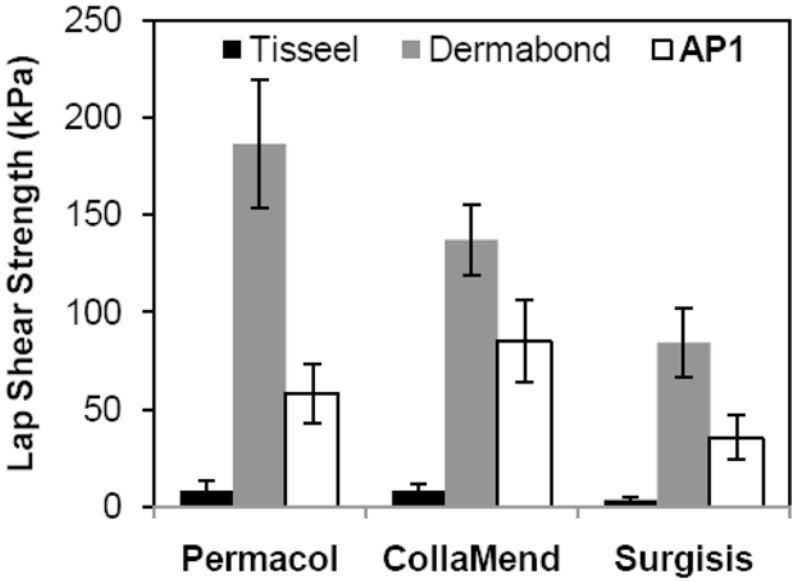

Figure 6.
Lap shear adhesive strength required to separate adhesive joint formed using adhesive-coated biologic meshes. For each mesh type, the adhesive strength of **AP1** differed significantly from that of the two commercial adhesives ($p < 0.05$).

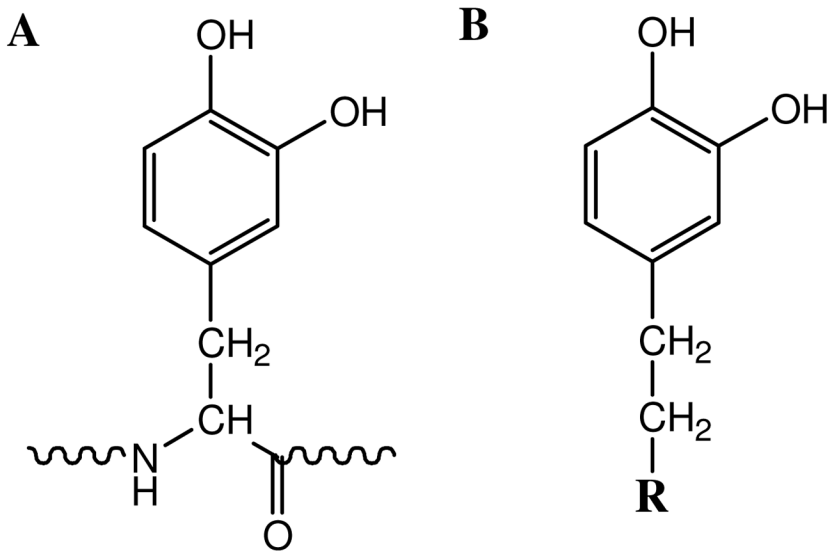

Figure 7.
Chemical structures of **A**) DOPA and **B**) DOHA (**R** = COOH) or dopamine (**R** = NH_2)

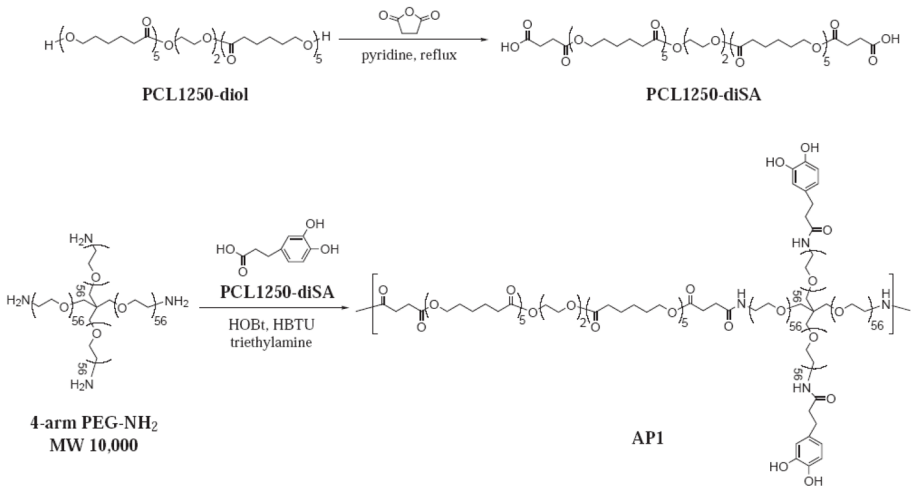

Scheme 1.
Synthesis scheme of **PCL1250-diSA** and **AP1**.

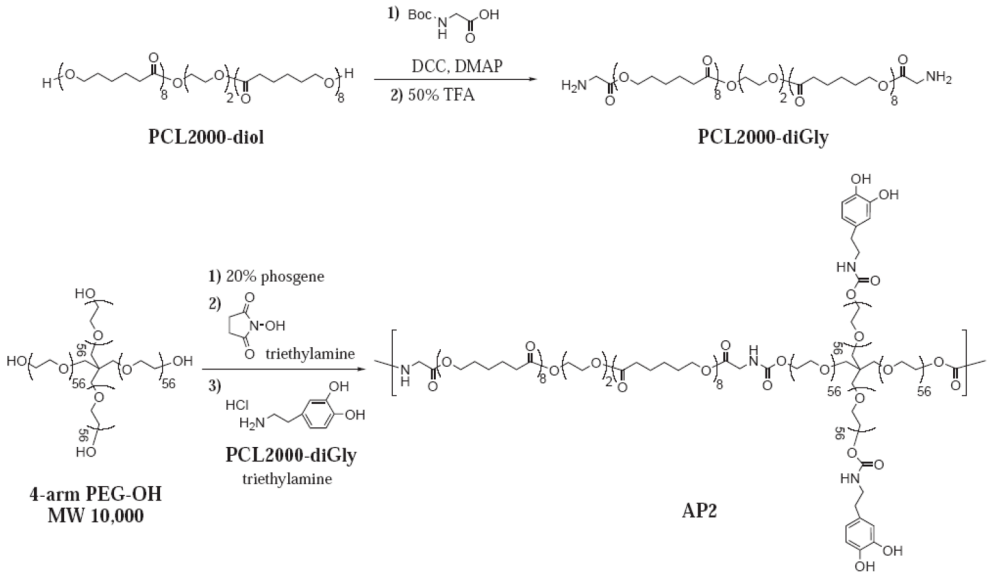

Scheme 2.
Synthesis scheme of **PCL2000-diGly** and **AP2**.

Table 1

Composition of the adhesive polymers.

Adhesive Polymer	Polymer Composition (wt%)				Catechol Type	GPC	
	^{1}H NMR			UV-vis			
	PEG	PCL	Catechol	Catechol		Molecular Weight (M_w)	PD*
AP1	84.0	13.4	2.6	3.1 ± 0.30	DOHA	98,000	2.8
AP2	76.6	20.6	2.8	3.4 ± 0.11	Dopamine	66,000	4.4

*Polydispersity (PD) = weight average molecular weight (Mw)/number average molecular weight (Mn)

Table 2

Equilibrium swelling of adhesive films.

Adhesive Polymer	Coating Density (g/m^2)[#]	Weight % PCL	Swollen Film Thickness (μm)[$]	Extent of Swelling (W_s-W_i/W_i)[*]
AP1	23	0	263 ± 9.64	9.8 ± 0.90
	46	0	368 ± 4.58	7.2 ± 0.61
	46	30	260 ± 40.1	4.2 ± 0.50
AP2	23	0	189 ± 4.51	7.0 ± 0.20
	46	0	261 ± 11.9	5.0 ± 0.20
	46	30	209 ± 6.66	4.2 ± 0.20

[#] Amount of polymer used to form the dry film in mass per unit area of the mold

[$] Measured with electronic micrometer

[*] For each polymer type, the mean values for each treatment are significantly different from each other ($p < 0.05$)

Table 3

Tensile properties of swollen adhesive films.

Adhesive Polymer	Weight % PCL	Young's Modulus (kPa)	Maximum Strength (kPa)	Strain at Failure	Toughness (kJ/m^3)
AP1	0	142 ± 37.6	168 ± 31.0	1.70 ± 0.403	168 ± 38.6
	30	103 ± 57.7	135 ± 51.6	1.95 ± 0.491	162 ± 77.3
AP2	0	219 ± 40.8	251 ± 21.2	1.82 ± 0.217	266 ± 29.1
	30	235 ± 58.1	357 ± 37.5	2.73 ± 0.337	562 ± 93.1

Vertical lines = statistical equivalence ($p > 0.05$)

Table 4

Effect of $NaIO_4$ concentrations on adhesive properties[#]

$NaIO_4$ Concentration (mg/mL)	Maximum Strength (kPa)	Work of Adhesion (J/m^2)[%]	Strain at Failure
10	9.34 ± 2.89[*]	22.2 ± 12.3[$]	0.489 ± 0.439
20	46.6 ± 19.3	77.0 ± 26.1[$]	0.366 ± 0.0698
30	42.3 ± 26.1	60.7 ± 34.5	0.315 ± 0.0627
40	45.0 ± 20.4	60.8 ± 14.6	0.168 ± 0.118

[#] Performed using **AP1**-coated bovine pericardium

[%] Normalized by initial area of contact

[*] Significantly different from other 3 treatments ($p < 0.05$)

[$] Significantly different from each other ($p < 0.05$)

Table 5

Effect of polymer coating density on adhesive properties[#]

Loading Density (g/m^2)	Maximum Strength (kPa)	Work of Adhesion (J/m^2)[%]	Strain at Failure	Burst Pressure (mmHg)
15	18.9 ± 5.41	33.2 ± 5.48	0.432 ± 0.201	———
30	31.7 ± 12.5	77.9 ± 35.5	0.494 ± 0.0997	219 ± 116
60	42.5 ± 12.3	91.6 ± 24.1	0.428 ± 0.0684	422 ± 136
90	37.9 ± 11.5	94.4 ± 42.2	0.422 ± 0.0543	495 ± 174

[#]Performed using **AP1**-coated bovine pericardium

[%]Normalized by initial area of contact

Vertical lines = statistical equivalence ($p > 0.05$)

Table 6

Effect of PCL-triol content on adhesive properties of **AP1**

Wt% PCL-triol	Maximum Strength (kPa)	Work of Adhesion (J/m^2)	Strain at Failure
0	70.0 ± 9.50	77.7 ± 13.3	0.293 ± 0.0498
15	88.4 ± 20.1	117 ± 15.8	0.469 ± 0.191
30	74.6 ± 29.3	131 ± 51.2*	0.481 ± 0.160

*Significantly higher than 0 wt% PCL-triol ($p < 0.05$).

Table 7

AP1coating thickness and weight on each biologic mesh

Mesh Type	Coating Thickness (μm)*	Coating Mass (g/m^2)#
Permacol	22	66
CollaMend	86	66
Surgisis	34	73

*Determined from the difference between the average thicknesses of coated and uncoated meshes as measured by a digital micrometer (n=6)

#Determined from the difference between the average mass densities of coated and uncoated meshes as measured by a balance (n=6)